Thermal Science and Engineering Progress 37 (2023) 101572

Contents lists available at ScienceDirect

Thermal Science and Engineering Progress

journal homepage: www.elsevier.com/locate/tsep

Adsorption energy system design and material selection: Towards a holistic approach

Emanuele Piccoli [a,b,*], Vincenza Brancato [c], Andrea Frazzica [c], François Maréchal [b], Sandra Galmarini [a,**]

[a] Empa, Ueberlandstrasse 129, 8600 Duebendorf, Switzerland
[b] EPFL, Rue de l'Industrie 17, 1950 Sion, Switzerland
[c] CNR-ITAE, Salita Santa Lucia Sopra Contesse 5, 98126 Messina, Italy

ARTICLE INFO

Keywords:
Material characterization
Adsorption equilibrium
Performance estimation
Optimization

ABSTRACT

The deployment of adsorption cycles for heating and cooling purposes is often limited by poor efficiency and high reactor volumes, both determined by the adsorber material used. The appropriate pre-selection of the solid sorbent and the system design in the early stages of design can allow quick identification of the most promising solutions. In this work, a reliable and robust methodology for adsorber material screening and pre-selection is proposed and applied to a test set of state-of-the-art candidates. The improvement achieved in the adsorption equilibrium prediction with respect to the most frequently used model is above 60%. In addition, the adsorber material selection framework based on mixed-integer linear programming was applied to over 600 hypothetical cooling and mixed cooling/heating use cases. The analysis of exergy and volume performances allowed to emphasize differences of design strategies using different system objectives (i.e. minimizing the temperature of the heat sources and choosing compact materials). We provide the proof of feasibility of a harmonic pre-design of adsorbent materials and energy system and show that it can be used to narrow down the decision variables to the most promising options. This methodology can be considered as the foundation of more extended and automated design methods for real scenarios constrained by kinetics, material integration and costs.

1. Introduction

Adsorption energy technologies can play an important role in making energy systems more sustainable [1,2]. Cooling, heating, and energy storage systems can be more efficient using the full potential of adsorbent materials, which allows for providing those services requiring little electricity (i.e. only auxiliary systems like valves and pumps). Nonetheless, several factors are limiting their widespread application, including low thermal efficiencies and large volumes when compared to competing solutions [3].

The performance of adsorption equipment strongly depends on the adsorbent–adsorbate working pair, and because of that, it is highly sensitive to the operational conditions (i.e. temperature, pressure) [4]. The pre-selection of the appropriate working pairs in the early stage of the design – before prototyping, testing and optimizing the equipment – can therefore enable competitive applications [5] at minimum time and costs for R&D. This can be achieved by characterizing the equilibrium thermophysical properties of the materials. These measurements demand only small amounts of material and allow the estimation of the maximum achievable thermal energy performance, identifying the most suitable adsorbents [6]. While these quantities do not take into account the kinetics of the adsorption process, no good performance can be reached without suitable equilibrium properties. Additionally the kinetics depend heavily on the heat exchanger design and will need either measurements on prototypes or advanced modelling. The adsorbent–adsorbate working pair is not the only driver of the adsorption heat transformer performance, but it is considered as a preliminary requirement. In fact, other aspects as material integration, heat exchanger design and control are similarly relevant. However, their optimization is not so dependent on the working pair obtained and can be included in later stages of the system design.

Being such an important step in the development of adsorption heat transformer, several approaches for material selection were already developed. Specifically Aristov and colleagues played a central role in developing the field. In [7] they considered the dynamic characterization and optimization of materials as the key indicator performance.

* Corresponding author at: Empa, Ueberlandstrasse 129, 8600 Duebendorf, Switzerland.
** Corresponding author.
E-mail addresses: emanuele.piccoli@empa.ch (E. Piccoli), sandra.galmarini@empa.ch (S. Galmarini).

https://doi.org/10.1016/j.tsep.2022.101572
Received 5 July 2022; Received in revised form 18 November 2022; Accepted 22 November 2022
Available online 25 November 2022

Nomenclature

Acronyms

$Al-fum.$	Aluminium Fumarate from MOF Technologies
$Al-iso.$	Aluminium Isophthalate from MOF Technologies
AC	Activated Carbon
$AQSOA-Z02$	AQSOA-Z02 from Mitsubishi Plastics
ATL	Averaged Temperature Lift
COP	Coefficient Of Performance
DA	Dubinin–Astakhov
EN	Energy use
EX	Exergy use
EV	Energy-specific Volume
$MILP$	Mixed Integer Linear Programming
MOF	Metal-Organic Framework
MSE	Mean Square Error
NU	Normalized use (of energy/exergy)
OBJ	Objective function
$RDSilicaGel$	RD Silica Gel from Fuji Davison
$RMF-AC$	Resorcinol–Melamine–Formaldehyde AC from Empa
RSE	Residual Standard Error
$SAPO-34$	SAPO-34 from Fahrenheit
$Siogel$	Siogel from Oker Chemie
SEM	Scanning Electron Microscopy
AHT	Adsorption Heat Transformer
$R\&D$	Research and Development
PSA	Pressure Swing Adsorption

Symbols

C	Characteristic energy of adsorption [J/g_w]
cp	Specific heat capacity [J/g/K]
F	Specific work of adsorption [J/g_w]
f	Degrees of freedom of the model
H	Specific heat of adsorption [J/g_w]
k	Total number of points predicted
M	Molar weight of water [g/mol]
n	Adsorption exponential shape factor [−]
L	Latent heat of evaporation of water [J/g_w]
p	Pressure [mbar]
R	Ideal gas constant [J/mol/K]
s	Size of the unit [−]
T	Temperature [K]
t	Time [s]
Q	Energy stream [J]
w	Specific adsorbed water loading [g_w/g_s]
W_0	Specific adsorbed water at saturation [g_w/g_w]
ϵ^2	Squared residuals
ρ	Density [g/cm3]
τ	Characteristic time [s]
δ	Dirac delta function
N	Number of elements
d	Particle size [mm]
Δ	Difference

Sub- and super-scripts

ad	Adsorption
c	Critical point of water
con	Condenser
de	Desorption
env	Environment
eva	Evaporator
fi	Final
hot	Hot source of the cycle
$train$	Training data
$cool$	System's cooling demand (also level)
$sink$	System's heat sink (also level)
$V50$	Volumetric median
tap	Tap (density)
$test$	Test data
i,k	Elements of the sums
in	Initial
max	Maximum
$need$	Energy need/requirement of the system
s	Solid adsorbent
sat	Saturation
T	Temperature level
w	Water
$param$	Model parameter
$heat$	System's heating demand (also level)
$source$	System's heat source (also level)
$switch$	Switching point between isosteric and isobaric adsorption
l	Level
$lift$	Temperature lift from evaporator to condenser
reg	Regeneration temperature lift from condenser to hot source

In [8], they recognized the importance of adsorbent databases as the foundation for comprehensive and quantitative evaluation of the existing water adsorbents. Nowadays, with the computational power growing unprecedentedly also within the scientific community, such databases are becoming even more important and are currently being maintained [9]. In [10] they reviewed the most promising classes of materials being developed and systematically exposed their pros and cons. More recently [11], they highlighted how adsorption cycles and materials should be developed harmoniously to maximize the thermodynamic synergy among them in both first-law and second-law terms.

Moreover, more authors have been contributing the development of the field. In [12], several working pairs have been simulated for different working conditions, providing insights on how to achieve maximum performance improving the cycles with heat recovery. In [13], several working pairs are evaluated and compared for different types of heat storage applications. In [14], modelling and simulations of several working pairs was used as a method to design systems considering both thermodynamic and dynamic aspects. In [15], a fingerprint method is proposed to evaluate a give material with two different driving temperatures as representative of different classes of applications. In [16], the adsorption isotherms extracted from a database are used to calculate theoretical coefficient of performance for a cooling and a heating cycle. In [17], a screening over a large number adsorbent–adsorbate of working pairs was computed for heating and cooling applications, with fixed evaporator and adsorption temperatures but with free desorption

temperature. In their work, both thermodynamic and heat transfer considerations are used as a selection criteria.

An important common aspect of all these works is the evaluation of the properties of the investigated adsorbents, especially regarding equilibrium and dynamic adsorption data. As special interest is often dedicated to water as adsorbate fluid [14], many studies concerned the water adsorption characteristics for relevant conditions [3]. When comparing different materials from a thermodynamic standpoint, water adsorption curves are used as a primary indicator and to feed models and simulations [18–21]. Models have been extensively used to understand and predict the amount of water adsorbed on a material surface in a given condition in the last century. Some of these models were applied to many different classes of nanoporous materials, due to their simple formulation. Among them, one should certainly cite the Langmuir model, the Sips model, the Toth model, the UNILAN model and the Dubin–Astakhov model [22,23]. In particular, the latter [24] is able to describe adsorbents with an S-shaped adsorption characteristic, which happens to be advantageous in heat transformers [16,25], and it is based on a single driving force, the potential energy of adsorption. The energy and entropy of adsorbed water may deviate from this theory, being dependent on temperature [26]. However, it is generally found that this description gives a good approximation of the first-order effects. Furthermore, a single D-A equation is representative of a uniform pore size distribution around a well-defined diameter, while in many commercial and novel adsorbents more than one pore type can contribute to the total adsorption [27,28]. This limitation, depending on the nature of the adsorbent material, might be more difficult to cope with, especially when characterizing over broad ranges of the potential energy of adsorption. In fact it is sometimes overcome with artefacts such as the segmentation of the fitting equation or the application to a limited range of water pressures [6]. An alternative route to model adsorption on heterogeneous surfaces is to generalize existing models. In [29], the adsorption happening at different thermodynamic conditions in different adsorption sites following the Langmuir model are summed with a probability factor.

In the field of pressure swing adsorption (PSA) systems for gas separation, optimization methods have already been used to optimize the design decisions. Those included the system design and operation [30–33]. In the field of adsorption heat transformers, the optimization often consisted in parameter sweeps, as for example in [34] where a dynamic model is used to optimize the design and the control of an adsorption chiller with two different adsorbent materials.

Analysing the state-of-the-art research some considerations can be taken:

- Experimental data on adsorbent material properties are needed to estimate the performance of AHT;
- Automated screening from a database of materials is possible and enables novel solutions;
- The description of adsorption characteristic in a general way is necessary to analyse generally unknown materials;
- Equilibrium properties can be sufficient to narrow-down the selection of the materials to the feasible candidates (and dynamic considerations are necessary afterwards);
- The feasibility of complex adsorption system can be studied with optimization algorithms.

In this work, we intend to fill some of the gaps necessary to estimate the feasibility of complex water-based adsorption heat transformers systems in a preliminary stage. In fact, by selecting at the same time materials and system design, the maximum benefits can be obtained. In a preliminary phase of the design, it is not worth to measure the kinetic performance of tens (and even less of hundreds or of thousands) of adsorbents under many different conditions, so one must rely on as little data as possible. Here a simple formulation for the maximum equilibrium performance is used to estimate the achievable energy and exergy efficiency and the minimum volume necessary. This estimation relies heavily on the water adsorption characteristic, therefore we propose a measuring and modelling solution to minimize the errors deriving from the extrapolation of those characteristics. Having such a simple description of the performance of the system, a simple optimization algorithm based on algebraic equations will be sufficient to demonstrate the feasibility of the approach, leaving a more detailed application of the methodology for later stages of design (including dynamic considerations and more representative process functions).

A similar effort was undertaken by Boman and colleagues [17]. However, some important differences between their approach and the one here proposed can be found. Those differences concern the use and validation of a more general and detailed adsorption model, and the simultaneous choice of material and system design.

Therefore, a new methodology for screening adsorbents for water as refrigerant fluid is reported, taking into account both the characterization and selection criteria. The aims include:

- a more accurate estimation of the maximum thermal performance;
- a robust method to identify the best adsorbent material depending on the temperature boundaries;
- a methodology that applies to a wide range of materials with very different characteristics;
- a methodology that could be expanded and automated to find optimal designs when connected to a database of materials properties.

This has been achieved by:

- introducing a novel model to describe the equilibrium adsorption characteristics;
- applying Mixed Integer Linear Programming (MILP) techniques as a tool for material selection;
- testing the methodology by estimating the maximum energy performance of a range of adsorber materials of different type, shapes and formats (state-of-the-art silica gels, zeo-types, Metal-Organic Frameworks (MOFs) and activated carbons (ACs)) for different heating and cooling scenarios.

We will first describe the methods and modelling approach in detail, namely the experimental measurements, the fitting of the equilibrium water sorption as well as the optimization approach. This will be followed by a discussion of the results. First we will be discussing the measured properties (density, heat of adsorption and adsorption isotherm) as well as the fitting of the equilibrium adsorption, ending with a discussion of the results of the optimization framework and some conclusions.

2. Materials and methods

2.1. Materials

Six adsorbent materials have been selected by virtue of their adsorption characteristics: two amorphous silica gels beads (Fuji Davison RD Silica Gel and Oker Chemie Siogel), adsorbing water over a wide range of relative pressures; two zeo-types (SAPO-34 powder from Fahrenheit and AQSOA-Z02 beads from Mitsubishi Plastics), adsorbing at low relative pressures; two MOF pellets (MOF Technologies Al-OH Fumarate and CAU-10-H) and one monolithic AC (developed in-house at Empa) adsorbing at intermediate relative pressures.

The RD silica gel from Fuji Davison are irregular granules with an average size of 0.84 mm. The Siogel from Oker are round beads with an average diameter of 1.1 mm. The SAPO-34 powder from Fahrenheit is an irregular powder with an average size of 0.025 mm. The AQSOA-Z02 from Mitsubishi Plastics are round beads with an average diameter of 2 mm. The Aluminium Fumarate and Aluminium Isophthalate from

MOF Technologies are elongated, quasi-cylindrical pellets, with average dimensions 1.9 × 3.8 mm and 1.5 × 3.7 mm, respectively. The Resorcinol–Melamine–Formaldehyde activated carbon from Empa is a shapeable monolith with integrated macroporosity.

2.2. Material characterization

In order to compute first-law thermodynamic analysis on potential adsorbent materials, some of their thermophysical and structural properties must be characterized, namely specific heat capacity, water adsorption isotherms, specific heat of adsorption, and tap density.

To calculate the energy the sensible heat spent during each cycle to heat up and cool down the adsorbent, specific heat capacity has been measured on dry samples by differential scanning calorimetry using a Mettler Toledo DSC 1 instrument, available at CNR/ITAE, following the standard method DIN 51007. The accuracy of the method is ±2%. However, it should be noted how, due to the different formats of the studied adsorbent candidates (powders, beads, monoliths; see Fig. 1), the achieved thermal contact during thermal characterization is not uniform. When comparing the obtained values for specific heat capacity this should be kept in mind. For the same reason, for the specific heat of sorption, the simplified theoretical value [6] $H = L(T) + F(T, p)$ was preferred to experimental values $H = H(w)$.

Water adsorption isotherms are fundamental to calculate the heat released/absorbed during the adsorption/desorption process and the sensible heat spent during each cycle to heat up and cool down the adsorbed phase. This property is the main indicator for ranking adsorbent materials and the most complex to model, as it will be detailed further below. For this reason, for each material multiple isotherms at temperatures between 10 °C and 80 °C were measured with an SMS DVS Endeavour and a TA Instruments VTI-SA+, available at Empa. More details about the characterization protocol used can be found elsewhere [35]. Adsorption and desorption isotherms of Oker Siogel, Fuji Silica gel, Fahrenheit SAPO34, Mitsubishi AQSOA Z02 granules, RMF-AC, CAU-10-H and Al(OH) fumarate were measured with a SMS DVS Endeavour instrument, following the protocol reported in [35]. The measurement errors are in the order of 0.01 [g/g]. To improve the reproducibility of the measurements, the water isotherms were analysed according to the protocol produced in the framework of the Hycool project [35]. Each ad/desorption step is fitted to an exponential function ($w = w_{in} + \Delta w_{max} * (1 - exp(\frac{t - t_{in}}{\tau}))$), where w and w_{in} are the current and initial loading, Δw_{max} is the equilibrium uptake for the step, t_{in} and t are the initial and the current time, and τ is the characteristic response time of the system using the Nelder–Mead method [36] as implemented in R. If most of the steps were interrupted after reaching 95% of the equilibrium loading change ($t - t_{in} > 3\tau$), the experiment was considered successful and the data accepted. This systematic control leads to a significant improvement in the reproducibility of the adsorption curves, reducing scatter and allowing a more reliable interpretation of the results. For duplicates on 30 °C and 50 °C isotherms of Oker Siogel, RMF-AC and Fahrenheit SAPO34, the maximum deviation between isotherm points, considered valid within the limit of the a-posteriori validity check mentioned and with the same relative humidity was ±0.02 [g/g].

To have realistic information about the volume of adsorption heat transformers, the effective density of the materials must be characterized as well. Tap density, which depends not only on the material structure, but also on its format, was measured on a Jolting volumeter JEL STAV II, available at Empa. The dried material is put into a cylinder and weighed. The sample will be tapped in multiple rounds until the difference in volume between two consecutive round is less than 2%, according to the American Standard ASTM D7481-18. The ratio of the sample mass and filled cylinder volume is the tap density. The size of the measurement cylinder was chosen in function of the particle size of the powder/granules measured, as the particle size (d_{V50}) has to be much smaller than the size of the cylinder to avoid surface effects (d_{V50} [mm] * 125 < cylinder volume [mL]).

2.3. Water adsorption equilibrium modelling

For the characterization of equilibrium adsorption and desorption of the selected materials at different temperatures, two different adsorption models were considered. The first is the widely applied Dubinin–Astakhov (DA) modelling approach [24,37]. The DA model has been developed for non-polar adsorbates and adsorption materials with a uniform pore size distribution. When water is used as adsorbate, the adsorption equilibrium should in general be expected to be temperature dependent [26]. Additionally, many of the studied adsorbent materials are characterized by multiple pore types, ranging from micropores to macropores. This can lead to an inaccuracies of the DA modelling approach [22]. Thus, an empirical modification of the DA model, accounting for up to two different pore types and an additional linear dependence of the DA parameters on temperature, is proposed, similarly to what was proposed in [38]. The aim of the modification was to increase the accuracy of adsorption equilibria prediction under different conditions, keeping at the same time the original generality.

As with the original DA approach, we assume the density of the water to be constant. However, as in [38], we allow for up to two different adsorption sites for every material (see Eqs. (1)–(2), where w_{ad} is the equilibrium adsorption water loading, W_0 is the maximum loading capacities, C is the characteristic energy of adsorption, n is characteristic of the width of the adsorption peak and F is the Polanyi adsorption potential, T the temperature, R the ideal gas constant and p_{sat} the saturation pressure and M the molar weight of the sorbate. The subscript 1 and 2 indicate the two adsorption sites.)

$$w_{ad} = W_{0,1} \cdot exp\left(-(F/C_1)^{n_1}\right) + W_{0,2} \cdot exp\left(-(F/C_2)^{n_2}\right) \tag{1}$$

$$F = \frac{R \cdot T}{M} ln(p/p_{sat}) \tag{2}$$

In addition to the above, all parameters $P \in (W_0, C, n)$ are considered to be potentially linearly dependent on temperature (Eq. (3)). This temperature-dependent description of the parameters allow for a more robust application of the model to materials for which the researcher does not know *a priori* the isotherm shape.

$$P = a_P \cdot T + b_P \tag{3}$$

To calculate the saturation pressure of water, we used the approximation reported by Wagner and Pruss [39] (Eqs. (4)–(5), where T_c and p_c are the temperature and pressure of the critical point of water respectively).

$$p_{sat} = p_c \cdot exp\left(\frac{T_c}{T} \cdot \left(-7.860 \cdot \nu + 1.844 \cdot \nu^{1.5} - 11.79 \cdot \nu^3 + 22.68 \cdot \nu^{3.5} - 15.96 \cdot \nu^4 + 1.801 \cdot \nu^{7.5}\right)\right) \tag{4}$$

$$\nu = 1 - T/T_c \tag{5}$$

Adsorption and desorption isotherms are in general different, and the difference between them is known as hysteresis. The hysteresis will significantly affect the amount of cyclable water under any conditions that do not encompass both the full adsorption as well as the full desorption peak. Geometrical and chemical features of the pores may determine the need for additional energy to desorb from certain sites (overcoming a bottleneck for example) [26,40]. As a consequence of such "delayed" desorption, the latter can be concentrated in a smaller range than during adsorption, leading to a higher desorption characteristic energy C and a modified shape n [41]. Depending on the material and the reason of the hysteresis, some physical model can be used to describe them. As in this work we do not focus on a specific type of hysteresis, instead of following the approach proposed in literature [41], it is preferred a general solution based on the curve fitting results. This can be expressed according to Eq. (6), where ΔC and Δn take into account the difference between ad- and desorption described

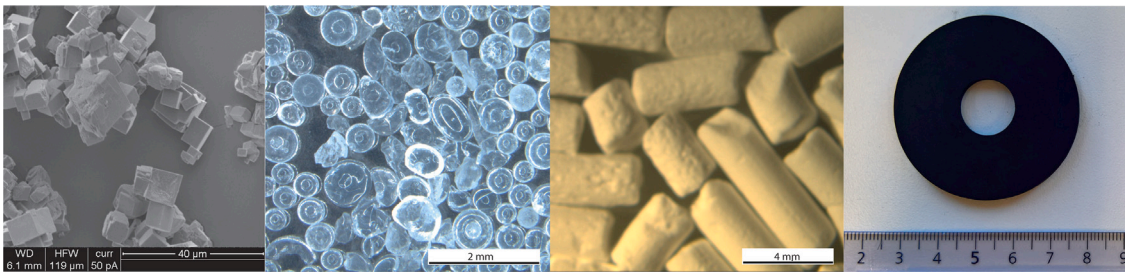

Fig. 1. Images of some of the characterized materials. From left to right, SEM of SAPO-34 from Fahrenheit, optical microscopy of Siogel from Oker and Aluminum Fumarate from MOF Technologies, picture of the Resorcinol–Melamine–Formaldehyde Activated Carbon from Empa.

above. The two terms describing hysteresis are also considered to be potentially linearly dependent on temperature (Eq. (3)).

$$w_{de} = W_{0,1} \cdot exp\left(-\left(\frac{F}{C_1 + \Delta C_1}\right)^{n_1+\Delta n_1}\right) + W_{0,2} \cdot exp\left(-\left(\frac{F}{C_2 + \Delta C_2}\right)^{n_2+\Delta n_2}\right) \quad (6)$$

2.4. Water adsorption equilibrium fitting

To ensure a good quality of the parameters describing the adsorption equilibria, and at the same time avoid over-fitting, a rigorous curve fitting procedure has been followed.

The obtained data was split using a stratification based on the total loading into a training set (80%) and a test set (20%), to have a more robust fitting in both areas of high loading and low loading. The random split was performed with the Python library *scikit-learn* [42].

The adsorption branch data were then fitted with both the original DA and the adapted model (Eqs. (1) and (3)). The optimal fit was obtained with the R library *nlrob* [43]. Subsequently, the parameters ΔC and Δn (Eq. (6)) were fitted on the desorption branches, using the same procedure. To ensure that for each material only the significant parameters are included in the final equation, when fitting the model parameters we followed the procedure below:

1. all the model parameters are included in the curve fitting;
2. the least significant of the parameters with a *p-value* > 0.05 is excluded;
3. if the overall quality of the model worsen, the parameter is restored and the second least significant is excluded;
4. The parameters are excluded until only the minimum number remains (either significant or necessary for the adsorption site to exist);
5. if two out of three parameters for each adsorption site distribution are significant, the distribution is kept, otherwise it is excluded.

This routine can ensure that only the most significant parameters are included in the fit. However, given the limited number of materials, it was performed manually and before its application to a wide database it should be automated.

2.5. Maximum theoretical performance estimation

While a precise analysis of the performance and the cost of adsorption heat exchangers can only be obtained through a dynamic analysis [44–47], for a first screening in the early stage of the design, the effort of constructing the lab-scale prototype necessary for such an analysis is excessive. From the measured equilibrium data, it is possible to calculate the maximum achievable energy performance of cooling cycles under well-defined working conditions [6]. While these values do not take into account any kinetic effects, a reasonable performance in terms of equilibrium properties is needed for a cycle to be efficient. Therefore, the maximum achievable energy performance is a good criterion for fast pre-selection of promising adsorption materials. For cooling applications the maximum theoretical thermal coefficient of performance (COP) – evaluating the ratio between delivered energy and thermal energy needed to drive the thermodynamic cycle – can be calculated as a function of the evaporator temperature T_{eva}, the adsorption temperature T_{con}, and the hot source temperature T_{hot} (Eq. (7), where L is the latent heat of vaporization of water). For an ideal cooling cycle, the transformations are either isosteric or isobaric [4].

$$COP = L(T_{eva}) \cdot \Delta w \cdot \left(\int_{T_{con}}^{T_{switch}} \left[cp_s(T) + cp_w(T) \cdot w(p_{eva}, T_{con}) \right] dT + \int_{T_{switch}}^{T_{hot}} \left[cp_s(T) + cp_w(T) \cdot w(p_{con}, T) - H_{de}(T) \cdot \frac{dw(p_{con}, T)}{dT} \right] dT \right)^{-1} \quad (7)$$

The temperature T_{switch}, at which the ideal desorption process switches from isosteric to isobaric is a function of the condensation (T_{con}) and evaporation (T_{eva}) temperatures [5] (Eq. (8)).

$$T_{switch} = \frac{T_{con}^2}{T_{eva}} \quad (8)$$

The energy (EN) and exergy (EX) use of the cycles can be respectively approximated as Eqs. (9) and (10).

$$EN = \frac{1}{COP} \quad (9)$$

$$EX = \frac{1}{COP} \cdot \left(1 - \frac{T_{env}}{T_{hot}}\right) \quad (10)$$

As a first indicator of reactor volume, at least in relative terms, the energy-specific adsorbent volume (in cm^3/J, Eq. (11)) can be used.

$$EV = \frac{1}{L(T_{eva}) \cdot \Delta w \cdot \rho_{tap}} \quad (11)$$

2.6. Formulation of the optimization problem

Finding the most advantageous solution to satisfy the heating and cooling loads of a specific energy system can be formulated as an optimization problem [48]. To this end, an objective function is defined and optimization is used to find the best values of the decision variables, within the limits of some constraints . This is also true for the number and type of adsorption materials used. Even though only equilibrium properties were considered within the current work, such optimization will allow a better understanding of how the decision variables (type and number of adsorber materials used) influence the objectives set (exergy, energy, volume) and should allow for a good pre-selection of materials.

To explore the possibilities of this approach, almost 700 feasible scenarios have been simulated. The scenarios have been created with cooling needs (goods and room cooling) during summer in Europe in mind (environmental temperature T_{env} = 30 °C), using a solar thermal heat source. The cooling needs can be complemented by a heating

need, either within industrial processes or for domestic hot water. Consequently each scenario has $1 \leq N_{cooling} \leq 5$ cooling demands $Q^{T_l}_{cooling}$ at temperatures $T_l \in \{5, 10, 15, 20, 25\ °C\}$ and can additionally have $N_{heating} \leq 5$ heating demands $Q^{T_m}_{heating}$ at a temperature $T_m \in \{35, 40, 45, 55\ °C\}$. The energy demands are normalized by an energy unit Δu (i.e. $Q^{T_m}_{heating} = Q'^{T_m}_{heating}/\Delta u$) and can only have discreet sizes of 1 or 2.

The number of adsorption heat transformers N_{AHT} used to meet the energy needs is part of the optimization. The ideal adsorption cycle of each adsorption heat transformer i is represented by three temperature levels ($T^i_{eva} < T^i_{con} < T^i_{hot}$, i.e evaporation, condensation and hot/desorption temperatures respectively). The temperature levels were restricted to the following ranges: evaporator between 5 °C and 25 °C; condenser between 15 and 55 °C; hot source between 25 °C and 95 °C, for simplification with discrete levels every 5 °C. Furthermore, each heat transformer is characterized by a size (s_i) and three energy streams associated with the three temperature levels ($Q^{T_k}_i$). Again the energy streams are normalized by an energy unit Δu ($Q^{T_k}_i = Q'^{T_k}_i/\Delta u$) such that for each adsorption heat transformer the evaporator stream is a unitary stream $Q^{T_{eva}}_i = 1$. The hot source stream is $Q^{T_{hot}}_i = -Q^{T_{eva}}_i/COP = -1/COP$, and the condenser stream is $Q^{T_{con}}_i = Q^{T_{eva}}_i \cdot (1 + 1/COP) = 1 + 1/COP$. The sign convention used is positive for energy streams entering the system (evaporators and hot sources), and negative streams for energy streams leaving the system (condensers). For each adsorption heat transformer, a different adsorber material can be chosen. The hot energy demands of the heat transformers $s_i \cdot Q^{T_{hot}}_i$ are met by external sources $Q^{T_{hot}}_{source}$ and energy exiting the system at temperatures above T_{env} can be ejected to environmental sinks $Q^{T_{con}}_{sink}$.

The systems thus defined is composed of a certain number of temperature levels $\{T_l\} = \bigcup_{i,k} T^i_k$, where $k \in \{cool, heat, sink, source\}$. For each temperature level T_l, an energy balance, defined in Eq. (12) using the Dirac delta function δ, has to be satisfied.

$$\sum_{i,k} \delta(T^i_k - T_l) \cdot s_i \cdot Q^{T_k}_i = \sum_{cool} \delta(T_{cool} - T_l) \cdot Q^{T_{cool}}_{cool} - \sum_{heat} \delta(T_{heat} - T_l) \cdot Q^{T_{heat}}_{heat} + \sum_{sink} \delta(T_{sink} - T_l) \cdot Q^{T_{sink}}_{sink} - \sum_{source} \delta(T_{source} - T_l) \cdot Q^{T_{source}}_{source} \quad (12)$$

Namely this energy balance implies, that the cooling and heating demands have to be met (Eqs. (13)–(14)).

$$\sum_{i,k} \delta(T^i_k - T_{cool}) \cdot s_i \cdot Q^{T_k}_i = -Q^{T_{cool}}_{cool} \quad (13)$$

$$\sum_{i,k} \delta(T^i_k - T_{heat}) \cdot s_i \cdot Q^{T_k}_i <= -Q^{T_{heat}}_{heat} \quad (14)$$

The objective function to minimize can be formulated in a similar way for both energy and exergy consumption, summing over energy/exergy of the heating/cooling cycle (according to Eqs. (9) and (10) respectively), counting only hot temperatures/heat sources above the environment temperature $T_{env} = 30$ °C.

$$OBJ_{EN} = \sum_{i \in \left\{ i | T^i_{hot} > T_{env} \right\}} s_i \cdot EN_i \quad (15)$$

$$OBJ_{EX} = \sum_{i \in \left\{ i | T^i_{hot} > T_{env} \right\}} s_i \cdot EX_i \quad (16)$$

In the case of minimum required volume, the objective function is summed over the volume of all adsorption heating/cooling cycles (Eq. (17)).

$$OBJ_{EV} = \sum_i s_i \cdot EV_i \quad (17)$$

The Python library *mip* [49] was used to optimize the choice and the connection of materials and boundary temperatures to deliver the cooling and heating needs of the system, according to the defined objective function. To speed up the optimization, the COPs of all materials and temperature levels T^i_k were pre-calculated.

Table 1
Material properties. Specific heat capacity is valid between 298 and 393 K.

Material	Specific heat capacity [J/g/K]	Tap density [g/cm^3]
Fuji Davison RD Silica Gel	$0.7 + 0.0019 \cdot (T - 273.15)$	0.87
Oker Chemie Siogel	$0.79 + 0.0016 \cdot (T - 273.15)$	0.77
Fahrenheit SAPO-34	$0.93 + 0.0063 \cdot (T - 273.15)$	0.85
Mitshubishi AQSOA-Z02	$0.84 + 0.0071 \cdot (T - 273.15)$	0.60
MOF Tech. Al-Fumarate	$0.97 + 0.0034 \cdot (T - 273.15)$	0.51
MOF Tech. Al-Isophthalate	$0.77 + 0.0086 \cdot (T - 273.15)$	0.33
Empa RMF Activated Carbon	$0.93 + 0.0063 \cdot (T - 273.15)$	0.43

3. Results and discussion

3.1. Heat capacity and density

The experimental specific heat capacity and tap densities are shown in Fig. 2 and summarized in Table 1, showing a good agreement with the data available in the literature [44,50–53], except for Empa RMF activated carbon that shows a higher specific heat capacity than typical commercial activated carbons. The specific heat capacity of water has been assumed to be $cp_w = 1.271e-5 \cdot T^2 - 8.170e-3 \cdot T + 5.493$ [54].

3.2. Equilibrium water adsorption

Each adsorbent material was characterized with at least three full isotherms (between 2% and 95% relative humidity) at three different temperatures (between 20 °C and 70 °C). The zeolites were characterized with an additional isotherm at 80 °C. Two isotherms of Siogel, SAPO-34 and RMF-AC were duplicated to check for reproducibility (due by the experimental method and by variations between samples). The reproducibility of the results could be significantly improved with an *a posteriori* equilibrium check and differences between duplicate measurements were ≤ 0.02 [g/g]. Taking into account larger variations due to differences in measurement methodology in different laboratories and variation between sample batches, a good agreement was found with other data published in literature [6,50,55–57]. The complete water adsorption isotherm data are made publicly available at [58].

The quality of the models has been evaluated according to the residual standard error RSE, which is the square root of the ratio between the sum of the squared residuals ϵ^2_i, and the degrees of freedom calculated from the number of observations/measured updates N_{train} and the number of parameters of the model N_{param} (Eq. (18)).

$$RSE = \sqrt{\frac{\sum \left(\epsilon^{train}_i\right)^2}{N_{train} - N_{param} - 2}} \quad (18)$$

The quality of the fitted curves was checked on the test set according to the mean square errors, obtained by dividing the sum of the squared errors by the total number of points N_{test} (Eq. (19)).

$$MSE = \frac{\sum \left(\epsilon^{test}_i\right)^2}{N_{test}} \quad (19)$$

The results of training set fitting and test set predictions of adsorption equilibria for the Dubinin–Astakhov (DA) model are shown in Fig. 3, while the same results for the proposed model are shown in Fig. 4. The fitted parameters of the proposed model for the adsorption branch are gathered in Table 2. The results of the proposed model for the desorption branches are shown in Fig. 5. The fitted parameters for the desorption branch are gathered in Table 3. The result metrics for both models and both adsorption and desorption are summarized in Table 4.

Looking at the differences between fitted and measured water uptake for the DA model (Fig. 3), one can see systematic deviation between fits and measurements. In addition with differences >0.1 [g/g], the scatter of the residuals is larger than the observed differences

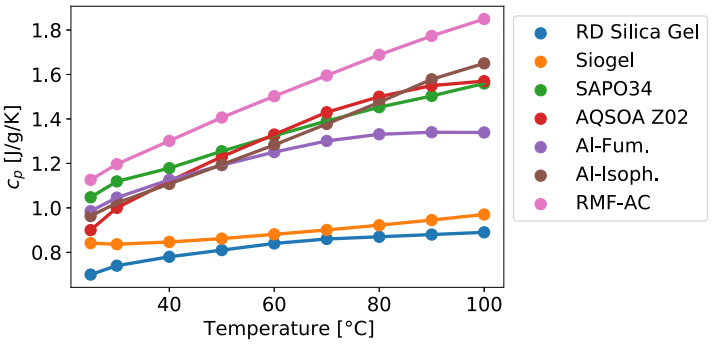

Fig. 2. Measured specific heat capacity of the adsorbent materials.

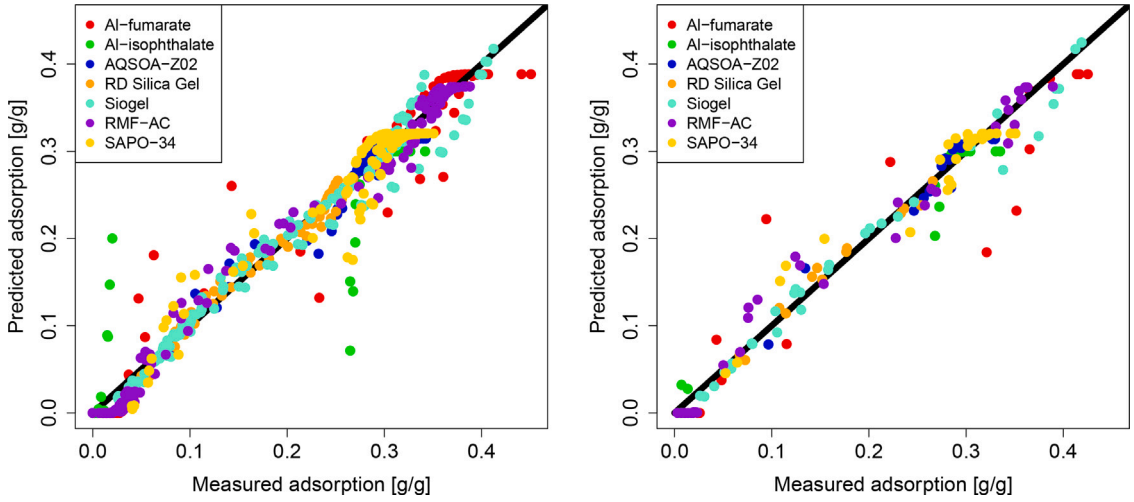

Fig. 3. Adsorption modelling results of the Dubinin–Astakhov model for the training data set (left) and for the test data set (right).

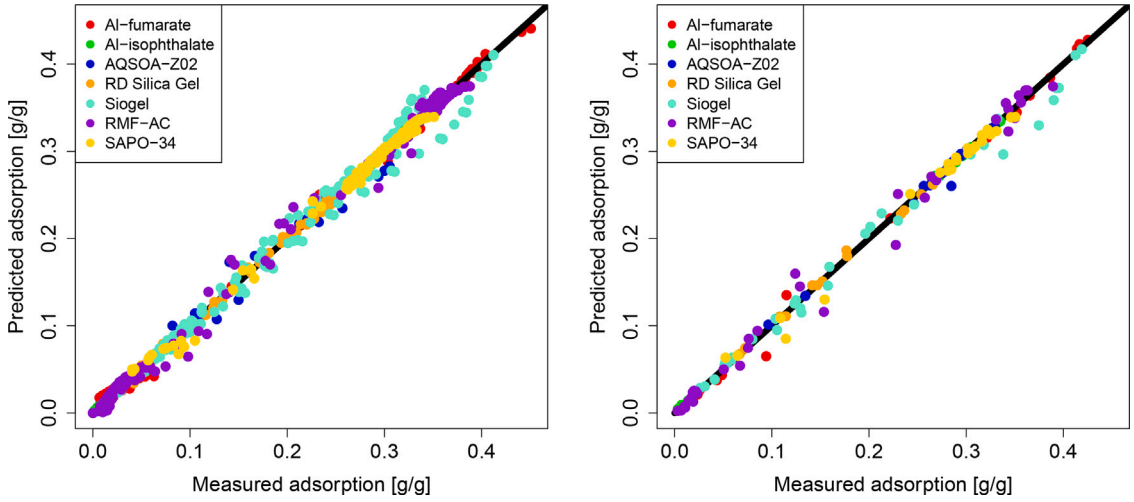

Fig. 4. Adsorption modelling results of the proposed model for the training data set (left) and for the test data set (right).

between duplicate measurements ($\leq$ 0.02 [g/g]). This indicates that water uptake predictions can be improved with a more adapted model.

With the adapted model chosen here (Eq. (1)), the three parameters of the DA model are replaced by minimum 6 and maximum 9 parameters (see Table 2). When comparing the standard DA model with the proposed empirical modification, the latter seems to provide a better of the equilibrium adsorption loadings, both with respect to accuracy and significance. The relative improvement achieved in model quality (residual standard error Eq. (18)) is normally between 60% and 87%. The only exception is OKER silica gel, which goes from the lowest residual standard error (1.2%) for the DA model to the highest (1.2%) for the new approach, thus showing no model quality improvement.

This general model improvement is reflected in better predictions, with an enhancement of the mean square error of 60% to more than 99%, the latter in the case of Al Isophtalate, which presents an almost perfect step-like isotherm (see Fig. 5). Interestingly, also for OKER silica gel, the predictions are greatly improved, highlighting an improved predictive capability of the new approach compared to the DA

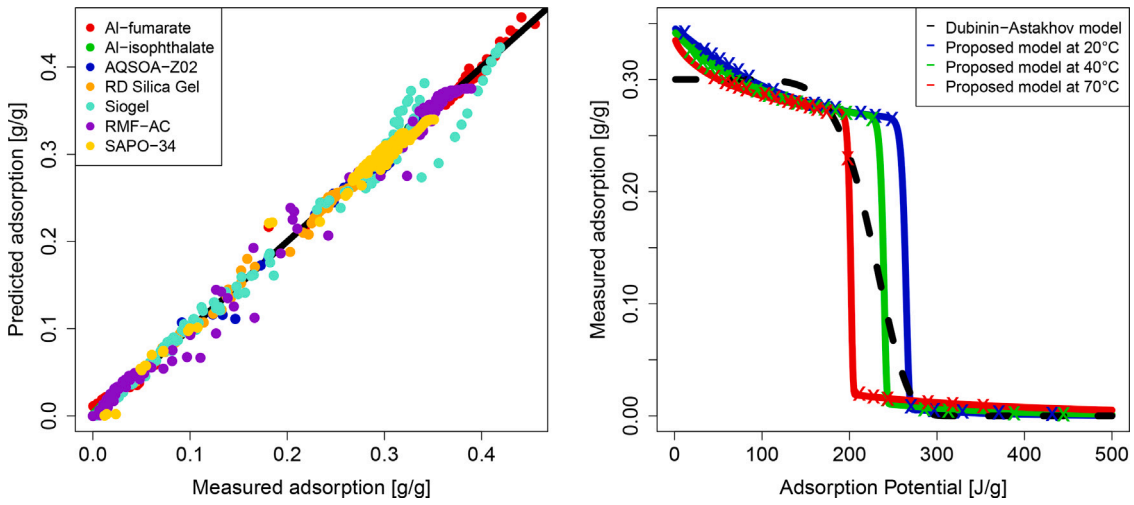

Fig. 5. Desorption modelling results of the proposed model for the training data set (left) and the difference between the Dubin–Astakhov model and the proposed model for the MOF Technologies Al-Isophthalate adsorption curve (right). For the latter, the X symbols represent experimental data.

Table 2
Proposed water adsorption model fitted parameters.

Code	$W_0 1$ [g_w/g]	$C1$ [J/g]	$n1$ [−]	$W_0 2$ [g_w/g]	$C2$ [J/g]	$n2$ [−]	N_{param} [−]
RD Silica Gel	$0.2 - 0.00032 \cdot T$	$260 - 0.32 \cdot T$	$0.01 \cdot T$	0.16	$710 - 0.92 \cdot T$	1.7	9
Siogel	$0.62 - 0.00086 \cdot T$	200	0.94	0.077	150	3.8	7
SAPO-34	0.15	500	1.4	$0.39 - 0.00067 \cdot T$	$910 - 1.8 \cdot T$	20	8
AQSOA-Z02	$0.088 + 0.00014 \cdot T$	$720 - 1.1 \cdot T$	$40 - 0.247 \cdot T$	0.26	620	0.4	9
Al-fumarate	$0.54 - 0.00073 \cdot T$	$490 - 0.96 \cdot T$	14	$0.001 \cdot T$	23	0.36	8
Al-isophthalate	0.087	110	$3.6 - 0.0085 \cdot T$	$0.3 - 0.00015 \cdot T$	$630 - 1.3 \cdot T$	$0.28 \cdot T$	9
RMF-AC	0.25	150	6.2	0.12	210	1.5	6

Table 3
Proposed water desorption model fitted parameters.

Code	$\Delta C1$ [J/g]	$\Delta n1$ [−]	$\Delta C2$ [J/g]	$\Delta n2$ [−]	N_{param} [−]
RD Silica Gel	13	$0.0092 \cdot T$	–	–	2
Siogel	$0.04 \cdot T$	0.11	$0.016 \cdot T$	32	4
SAPO-34	45	$0.0011 \cdot T$	$280 - 0.63 \cdot T$	$-0.017 \cdot T$	5
AQSOA-Z02	$169 - 0.32 \cdot T$	$92 - 0.25 \cdot T$	170	$0.29 - 0.00087 \cdot T$	7
Al-fumarate	$0.027 \cdot T$	$0.014 \cdot T$	$75 - 0.2 \cdot T$	0.044	5
Al-isophthalate	$0.028 \cdot T$	–	$170 - 0.5 \cdot T$	–	3
RMF-AC	–	1.4	21	$6.6 - 0.02 \cdot T$	4

Table 4
Water adsorption modelling results. RSEs are calculated over the train sets, while MSEs are calculated over the test sets.

Code	DA Ads. RSE	DA Ads. MSE	Own Ads. RSE	Own Ads. MSE	Own Des. RSE	Own Des. MSE
RD Silica Gel	1.1%	1.1e−4	0.4%	1.6e−5	0.6%	1.4e−4
Siogel	1.2%	3.3e−4	1.2%	2.1e−4	0.8%	4.4e−4
SAPO-34	2.1%	5.0e−4	0.3%	7.6e−5	0.9%	1.6e−4
AQSOA-Z02	1.4%	2.2e−4	0.2%	3.9e−5	0.2%	1.8e−5
Al-fum.	2.7%	5.2e−3	0.4%	3.6e−4	0.7%	2.2e−4
Al-iso.	1.5%	5.7e−3	0.2%	1.9e−6	0.2%	4.4e−4
RMF-AC	2.2%	4.9e−4	0.7%	1.9e−4	0.9%	9.7e−5

model, justifying the additional parameters. Constraining the desorption branch equation to have the same maximum loading capacities as the adsorption branch is, from the model fitting point of view, an additional constraint, resulting in a slightly higher mean squared error (average mean squared error of 2.16e−4 compared to 1.28e−4 for the adsorption branch). Nonetheless, the results of both the model fit and the predictions remain comparable to the reproducibility of the measurements, indicating a good fit.

Taking a closer look at the fitting results, one can notice how not all the materials have the same dependence on temperature. The Empa RMF activated carbon has an almost temperature-independent adsorption behaviour, which makes it characterization less vulnerable to misinterpretation (i.e. extrapolation of the curve to temperatures outside the characterization range). Other materials, such as Fuji RD Silica Gel and Al-Isophthalate, have a stronger temperature dependence.

During the fitting procedure, from one hand it was observed that only the inclusion of the temperature dependence of the model parameters could explain the differences observed between isotherms measured at different temperatures. On the other hand, it was observed that the most significant contribution to the improvement of the model predictions over the wide range of relative humidity here reported was due to the presence of an additional adsorption site (the second term of Eq. (1)). This means that if the experimental resources are scarce (e.g. the time available for the characterization of the adsorption

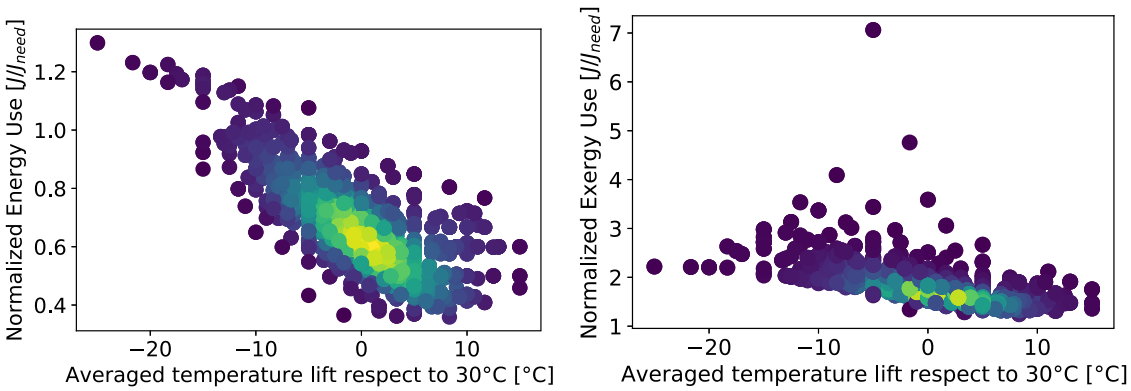

Fig. 6. Minimum normalized energy use (left) and exergy use (right) as a function of the averaged temperature lift. The colour of the points is scaled on the point density as a qualitative guide to the eye.

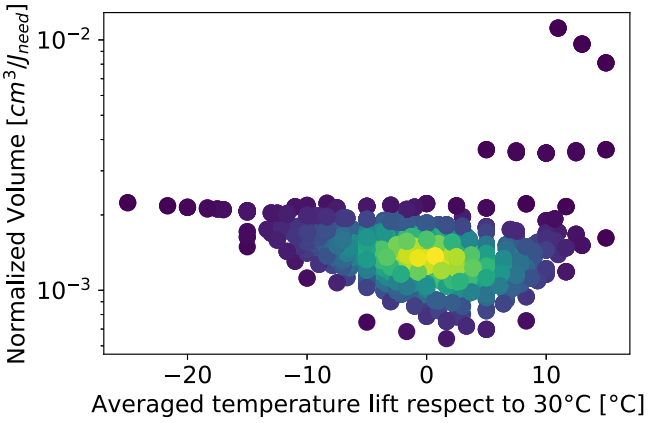

Fig. 7. Minimum normalized volume as a function of the averaged temperature lift. The colour of the points is scaled on the point density as a qualitative guide to the eye.

curves, or the temperature range available), it would still be possible to improve the D-A model even if the temperature effects are not detected in the measurement range. This approach, which coincides with the extension of [38] to include the desorption branches, would be suited for a quick scan of the adsorbent materials available, but at the risk of introducing errors. Those could be potentially extremely significant for materials characterized by step-like adsorption characteristics. In fact, the effects of temperature might shift the desorption peak towards different adsorption potentials. In Fig. 5 (right), the adsorption peak shift for Al-isophthalate can be easily observed.

3.3. Optimization

The maximum calculated cooling COP of the 212 possible, single, ideal cycles with temperature boundaries as described in the methods section ranged between 0.05 and 0.95, with most of the cycles between 0.75 and 0.85, in agreement with values found in literature [6,59]. The cycles performance have been pre-calculated to avoid calling the performance model from within the optimization algorithm, therefore lightening the computational effort required during the system design.

To show the applicability of the methodology to complex energy needs and to screen among materials to see which ones are more recurrently selected, the energy use, the exergy use, and the reactor volume objective functions were minimized for almost 700 scenarios, as described in the Methods section. As shown in Fig. 6, it was possible to achieve good system efficiencies for most of the scenarios. For analysing the results, the optimal solutions have been plotted against the averaged temperature lift (ATL) with respect to the environmental temperature T_{env} = 30 °C (Eq. (20)).

$$ATL = \frac{\sum_l Q_{need}^{T_{need}} * T_{need}}{\sum_{T_{need}} Q_{need}^{T_{need}}} - T_{env} \tag{20}$$

To compare scenarios with different amounts of energy needs, the normalized energy and exergy use (NU, Eq. (21)) are plotted.

$$NU = \frac{OBJ}{\sum_{T_{need}} Q_{need}^{T_{need}}} \tag{21}$$

As is expected, higher ATLs allow for better thermodynamic performance, including the ones that are generated as a combination of energy needs at different temperatures. Only in a few cases, the NU of energy was above 1.1 (for ATL <−15 °C) and the NU of exergy was above 3. Interestingly, the synergies among multiple heat transformers deliver NU of energy below one for ATLs below zero (ATL >−15 °C), showing the potential of harmonic material choice and system design.

It can also be noted how, for some scenarios of mixed heating and cooling (ATL between −5 and 10), extremely compact designs are achievable (theoretical minimum energy-specific volumes below 1 mm^3/J, see Fig. 7). This is the case when one adsorption heat transformer can provide cooling and heating at the same time, which means that the temperature levels are not far from each other (e.g. cooling at 15 °C and heating at 35 °C, with ATL of −1.7 °C). However, these scenarios are less likely to exist in the industry. The less compact outlayers at high ATL are due to the upper limit of 90 °C imposed on the regeneration temperature.

Looking at the composition of the optimal solutions, as in Fig. 8, it is possible to notice that most of the optimal solutions are composed of 3 to 5 adsorption heat transformers. Cascade configurations (where the condenser of one cycle feed the evaporator of another cycle) are beneficial when the energy needs happen at very different temperature (e.g. when cooling at 5 °C and heating at 55 °C are required, as in Fig. 10). While this highlights the options offered by combining AHTs, it also shows that the inclusion of cost functions in the optimization algorithm is necessary to avoid an over-population of AHTs, as it is known that manufacturing and equipment costs are an important share of the total costs [60].

When the energy consumption is being minimized, the majority of the adsorption heat transformers use Fahrenheit SAPO34 (for low adsorbate partial pressure cycles) and Al-fumarate (for intermediate adsorbate partial pressure cycles), proving that they are the most promising materials for the here studied scenarios. On average, Fahrenheit SAPO34 is used for temperature lifts ($\Delta T_{lift} = T_{con} - T_{eva}$) of 30 °C with a COP of 0.73, but requires a regeneration temperature lift ($\Delta T_{reg} = T_{hot} - T_{con}$) of 46 °C. On average, the MOF Tech. Al-fumarate is used for ΔT_{lift} of 20 °C and needs ΔT_{reg} of 32 °C, delivering a COP of 0.87. Most of the remaining cycles needed to balance the energy

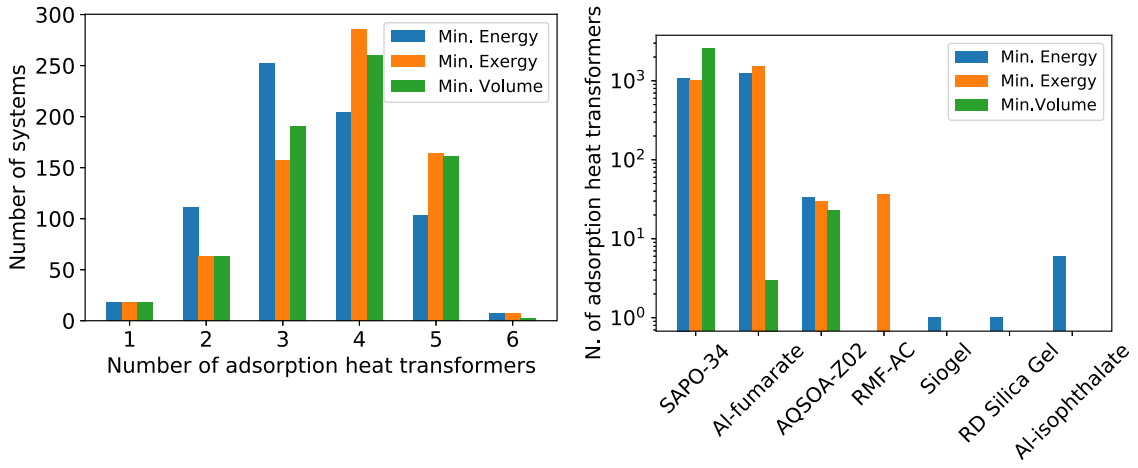

Fig. 8. The distribution of the number of adsorption heat transformers per system (left) and the adsorbent material candidates use (right) for energy and exergy consumption, and volume minimization.

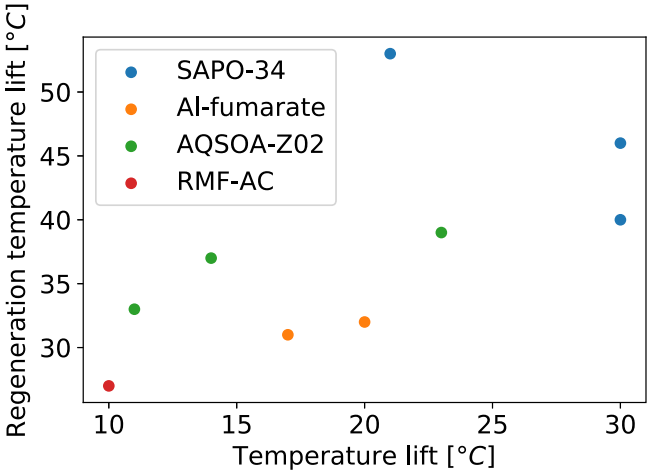

Fig. 9. Average use conditions (temperature lift provided during adsorption and regeneration temperature lift necessary during desorption) of the most selected materials: SAPO-34 from Fahrenheit, Al-fumarate from MOF Technologies, AQSOA-Z02 from Mitsubishi, RMF-AC from Empa.

needs are using Mitsubishi AQSOA Z02 beads, specifically on average for ΔT_{lift} of 11 °C and needing ΔT_{reg} of 33 °C, delivering a COP of 0.43.

Similarly, when exergy use is being minimized, Fahrenheit SAPO34 and MOF Tech. Al-fumarate are chosen the most. However, given the different objective, their average regeneration temperature lifts are reduced to 40 °C and 31 °C, respectively. The reported exergetic COP for these two materials and Mitsubishi AQSOA Z02 are 0.61, 0.80 and 0.31, respectively. In this case, the extremely narrow shape of adsorption curve (without hysteresis and temperature effects) of the Empa RMF Activated Carbon combined with its high adsorption capacity seem beneficial for exergetic performance, and this adsorbent is used when small temperature lifts are required (ΔT_{lift} of 10 °C and ΔT_{reg} of 27 °C), with an average exergetic COP of 0.83.

While these first two indicators are informative about the operational expenditure, having low running costs is often not enough, especially when competing with conventional heat pumps. In the scenarios minimizing the reactor volume, the figure for cycles at intermediate relative pressures change completely: the low density of the MOFs is too penalizing, and almost only the denser zeo-types are used. This emphasizes how a screening only based on the adsorption isotherms is not the most efficient, and some parameters representing the integration on the heat exchangers must be included. Using V_{EN} is a good first approximation, but it is important to keep in mind that different material formats (powders, granules, monoliths) provide different packing densities according to their shape and size distribution. More advanced stages of design would require the characterization of the materials as integrated on the heat exchanger and more complete thermodynamic and kinetic considerations, that can deeply change the results in favour of faster and practical-to-handle materials. As stated in the Introduction, those elements have to be ideally integrated in the harmonic design of adsorption energy systems, however they cannot be included when analysing materials as coming from the production factories and laboratories. For minimizing the energy-specific volume of the system, the most frequently selected material is Fahrenheit SAPO34, with average ΔT_{lift} of 21 °C, ΔT_{reg} of 53 °C and an energy density of 350 J/cm^3. Mitsubishi AQSOA Z02 is again mostly used to balance the energy needs, with average ΔT_{lift} of 23 °C, ΔT_{reg} of 39 °C and an energy density of 35 J/cm^3.

As a general consideration on the material selection methodology applied to simplified energy systems, it appears that the combination of “heavy-duty” materials such as zeo-types and “light-duty” materials such as MOFs and ACs is beneficial depending on the needs. The average working conditions chosen for the best materials are summarized in Fig. 9. Fahrenheit SAPO34 seems to be able to work in conditions that are more challenging for adsorption processes, such as high temperature lifts and limited regeneration temperatures. Despite its very interesting adsorption characteristic, the MOF Tech. Al-isophthalate cannot compete with the high water capacity of the Al-fumarate. It is also interesting to notice how the silica gels, despite their good adsorption capacity, are rarely a good choice because of the adsorption hysteresis and the broad adsorption peak, both limiting the actual cycled water.

Looking at specific scenarios is the goal of a screening performed by the system designer/developer interested in a specific application. In general, simple energy needs lead to simple solutions. For example, refrigeration at 5 °C is most energy-efficiently provided by a single adsorption cycle using Fahrenheit SAPO34 fed by a hot stream at 85 °C and discharging energy to a 35 °C condenser. This thermodynamically challenging solution has an ATL of −25 °C and an overall NU of energy of 1.3. The exergy minimization brings to the same choice, as the COP loss using lower-temperature hot streams is in this case too big. If the reactor must have the minimum possible volume, a hot stream temperature of 95 °C is preferred.

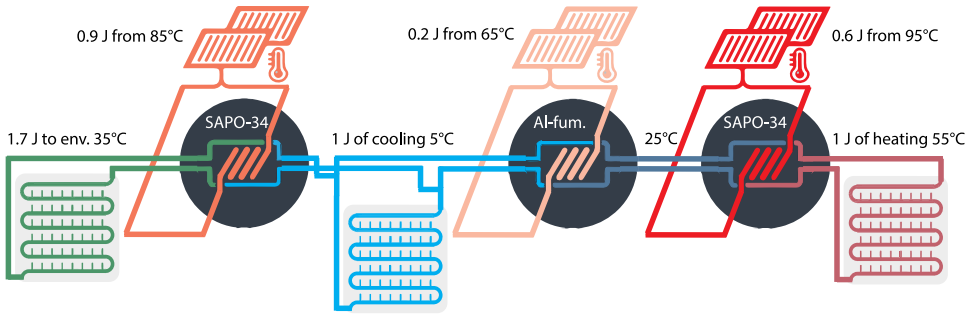

Fig. 10. Example of cascade configuration for mixed energy needs (cooling at 5 °C and heating at 55 °C, with minimum energy use). Part of the cooling needs are satisfied with a less efficient cycle using Al-fumarate, but gaining overall efficiency thanks to its synergy with the heating cycle.

If the energy needs are more diverse, such as in the case depicted in Fig. 10, having multiple reactors is more convenient. If the amount of cooling energy needed does not surpass the needs for heating, the minimum number of adsorption heat transformers is equal to the number of temperature levels of the energy needs. From the illustration, one can appreciate how the NU of energy is minimized thanks to the double use of the Al-Fumarate adsorption cycle. This combined heating and cooling scenario is characterized by an ATL of 0 °C and a NU of energy of 0.85.

The use of energy sources at different temperatures, often recurring in scenarios characterized by complex energy needs, adds some complexity to the system, for example spilling some of the hot streams from one reactor to another or having multiple heat generators. Anyway, it brings efficiency improvements also on the generator side (e.g. minimizing the fraction of solar collectors running at high temperatures).

4. Conclusions

In this work, a reliable and robust methodology to screen and preselect adsorbent materials for adsorption heat transformer systems was presented. The characterization of tap density, and of specific heat capacity and equilibrium water vapour sorption at different temperatures provided enough information to evaluate the maximum achievable performances of heating and cooling cycles for energy use, exergy use and volume required. In particular, measuring the adsorption curves over wide ranges of relative humidity and temperature is fundamental for extrapolating the results for simulation purposes.

The equilibrium adsorption data use was improved by the fitting of a novel empirical modification of the Dubinin–Astakhov model, that shows increased significance and accuracy with respect to the original. The effects of temperature and, especially, of multiple adsorption sites explain in an effective and general way the observed water adsorption behaviour.

Ideal adsorption cycles have been evaluated as a function of adsorbent temperature-dependent properties and target system temperatures only. This enables the evaluation of the suitability of adsorbent materials as coming from the manufacturer for given adsorption energy transformation applications. The simulation and optimization of different application scenarios allow for determining the most suitable adsorbent materials and system designs at the same time, potentially enabling high-performance solutions. In particular, the combination of zeolites for high temperature lifts and MOFs or ACs for smaller temperature lifts provided promising results.

In conclusion, the method presented here proved to be a powerful tool to help material, equipment and system developers to estimate the achievable performances, and to focus the R&D efforts only on the most attractive adsorbent materials. While contributing to the foundation of exhaustive adsorption energy systems design tools, this methodology should be further expanded to integrate a more appropriate performance evaluation, specifically including: kinetics, material integration on the heat exchangers, cost functions, realistic applications.

CRediT authorship contribution statement

Emanuele Piccoli: Conceptualization, Methodology, Software, Validation, Formal analysis, Investigation, Data curation, Writing – original draft, Writing – review & editing, Visualization. **Vincenza Brancato:** Validation, Investigation, Data curation, Supervision. **Andrea Frazzica:** Validation, Investigation, Data curation, Supervision. **François Maréchal:** Conceptualization, Supervision. **Sandra Galmarini:** Conceptualization, Methodology, Resources, Writing – original draft, Writing – review & editing, Visualization, Supervision, Project administration, Funding acquisition.

Declaration of competing interest

The authors declare the following financial interests/personal relationships which may be considered as potential competing interests: Emanuele Piccoli reports financial support was provided by European Commission.

Data availability

Data will be made available on request.

Acknowledgements

This work was performed in the framework of the project *HyCool: Industrial Cooling through Hybrid system based on Solar Heat*, funded by the European Commission H2020 Programme under Grant Agreement No. 792073.

References

[1] D. Sonar, S. Soni, D. Sharma, Micro-trigeneration for energy sustainability: Technologies, tools and trends, Appl. Therm. Eng. 71 (2) (2014) 790–796, http://dx.doi.org/10.1016/j.applthermaleng.2013.11.037, URL: https://linkinghub.elsevier.com/retrieve/pii/S1359431113008417.

[2] A. Ntiamoah, J. Ling, P. Xiao, P.A. Webley, Y. Zhai, CO_2 capture by temperature swing adsorption: Use of hot CO_2 -rich gas for regeneration, Ind. Eng. Chem. Res. 55 (3) (2016) 703–713, http://dx.doi.org/10.1021/acs.iecr.5b01384, URL: https://pubs.acs.org/doi/10.1021/acs.iecr.5b01384.

[3] H. Demir, M. Mobedi, S. Ülkü, A review on adsorption heat pump: Problems and solutions, Renew. Sustain. Energy Rev. 12 (9) (2008) 2381–2403, http://dx.doi.org/10.1016/j.rser.2007.06.005, URL: https://linkinghub.elsevier.com/retrieve/pii/S1364032107000998.

[4] M.M. Younes, I.I. El-Sharkawy, A. Kabeel, B.B. Saha, A review on adsorbent-adsorbate pairs for cooling applications, Appl. Therm. Eng. 114 (2017) 394–414, http://dx.doi.org/10.1016/j.applthermaleng.2016.11.138, URL: https://linkinghub.elsevier.com/retrieve/pii/S1359431116334809.

[5] Y.I. Aristov, Novel Materials for Adsorptive Heat Pumping and Storage: Screening and Nanotailoring of Sorption Properties, J. Chem. Eng. Jpn. 40 (13) (2007) 1242–1251, http://dx.doi.org/10.1252/jcej.07WE228.

[6] V. Brancato, A. Frazzica, Characterisation and comparative analysis of zeotype water adsorbents for heat transformation applications, Sol. Energy Mater. Sol. Cells 180 (2018) 91–102, http://dx.doi.org/10.1016/j.solmat.2018.02.035, URL: http://www.sciencedirect.com/science/article/pii/S0927024818300953.

[7] Y.I. Aristov, Optimal adsorbent for adsorptive heat transformers: Dynamic considerations, Int. J. Refrig. 32 (4) (2009) 675–686, http://dx.doi.org/10.1016/j.ijrefrig.2009.01.022, URL: https://linkinghub.elsevier.com/retrieve/pii/S0140700709000383.

[8] Y.I. Aristov, Adsorptive transformation of heat: Principles of construction of adsorbents database, Appl. Therm. Eng. 42 (2012) 18–24, http://dx.doi.org/10.1016/j.applthermaleng.2011.02.024, URL: https://linkinghub.elsevier.com/retrieve/pii/S1359431111001049.

[9] D. Siderius, NIST/ARPA-E database of novel and emerging adsorbent materials, Version 1.0.4, 2020. http://dx.doi.org/10.18434/T43882. URL: https://data.nist.gov/od/id/FF429BC1787D8B3EE0431A570681E858236.

[10] Y.I. Aristov, Challenging offers of material science for adsorption heat transformation: A review, Appl. Therm. Eng. 50 (2) (2013) 1610–1618, http://dx.doi.org/10.1016/j.applthermaleng.2011.09.003, URL: https://linkinghub.elsevier.com/retrieve/pii/S1359431111004832.

[11] L. Gordeeva, Y. Aristov, Adsorptive heat storage and amplification: New cycles and adsorbents, Energy 167 (2019) 440–453, http://dx.doi.org/10.1016/j.energy.2018.10.132, URL: https://linkinghub.elsevier.com/retrieve/pii/S0360544218321285.

[12] A. Frazzica, V. Palomba, B. Dawoud, Thermodynamic performance of adsorption working Pairs for low-temperature waste heat upgrading in industrial applications, Appl. Sci. 11 (8) (2021) 3389, http://dx.doi.org/10.3390/app11083389, URL: https://www.mdpi.com/2076-3417/11/8/3389.

[13] A. Frazzica, A. Freni, Adsorbent working pairs for solar thermal energy storage in buildings, Increasing the renewable share for heating and cooling by the means of sorption heat pumps and chillers, Renew. Energy 110 (2017) 87–94, http://dx.doi.org/10.1016/j.renene.2016.09.047, URL: http://www.sciencedirect.com/science/article/pii/S0960148116308370.

[14] A. Freni, G. Maggio, A. Sapienza, A. Frazzica, G. Restuccia, S. Vasta, Comparative analysis of promising adsorbent/adsorbate pairs for adsorptive heat pumping, air conditioning and refrigeration, Appl. Therm. Eng. 104 (2016) 85–95, http://dx.doi.org/10.1016/j.applthermaleng.2016.05.036, URL: https://linkinghub.elsevier.com/retrieve/pii/S1359431116306895.

[15] S. Henninger, F. Schmidt, H.-M. Henning, Water adsorption characteristics of novel materials for heat transformation applications, Appl. Therm. Eng. 30 (13) (2010) 1692–1702, http://dx.doi.org/10.1016/j.applthermaleng.2010.03.028, URL: https://linkinghub.elsevier.com/retrieve/pii/S1359431110001389.

[16] Z. Liu, W. Li, P.Z. Moghadam, S. Li, Screening adsorbent–water adsorption heat pumps based on an experimental water adsorption isotherm database, Sustain. Energy Fuels 5 (4) (2021) 1075–1084, http://dx.doi.org/10.1039/D0SE01824D, URL: http://xlink.rsc.org/?DOI=D0SE01824D.

[17] D.B. Boman, D.C. Hoysall, D.G. Pahinkar, M.J. Ponkala, S. Garimella, Screening of working pairs for adsorption heat pumps based on thermodynamic and transport characteristics, Appl. Therm. Eng. 123 (2017) 422–434, http://dx.doi.org/10.1016/j.applthermaleng.2017.04.153, URL: https://linkinghub.elsevier.com/retrieve/pii/S1359431116344283.

[18] A. Rezk, R. Al-Dadah, S. Mahmoud, A. Elsayed, Experimental investigation of metal organic frameworks characteristics for water adsorption chillers, Proc. Inst. Mech. Eng. C 227 (5) (2013) 992–1005, http://dx.doi.org/10.1177/0954406212456469, URL: http://journals.sagepub.com/doi/10.1177/0954406212456469.

[19] S.K. Henninger, F. Jeremias, H. Kummer, C. Janiak, MOFs for use in adsorption heat pump processes, Eur. J. Inorg. Chem. 2012 (16) (2012) 2625–2634, http://dx.doi.org/10.1002/ejic.201101056, URL: https://onlinelibrary.wiley.com/doi/10.1002/ejic.201101056.

[20] I. Jahan, T.H. Rupam, M. Palash, K.A. Rocky, B.B. Saha, Energy efficient green synthesized MOF-801 for adsorption cooling applications, J. Mol. Liq. 345 (2022) 117760, http://dx.doi.org/10.1016/j.molliq.2021.117760, URL: https://linkinghub.elsevier.com/retrieve/pii/S0167732221024855.

[21] L. Calabrese, L. Bonaccorsi, P. Bruzzaniti, A. Frazzica, A. Freni, E. Proverbio, Adsorption performance and thermodynamic analysis of SAPO-34 silicone composite foams for adsorption heat pump applications, Mater. Renew. Sustain. Energy 7 (4) (2018) 24, http://dx.doi.org/10.1007/s40243-018-0131-y, URL: http://link.springer.com/10.1007/s40243-018-0131-y.

[22] M. Llano-Restrepo, M.A. Mosquera, Accurate correlation, thermochemistry, and structural interpretation of equilibrium adsorption isotherms of water vapor in zeolite 3A by means of a generalized statistical thermodynamic adsorption model, (ISSN: 03783812) 2009, pp. 73–88, http://dx.doi.org/10.1016/j.fluid.2009.06.003, 283 (1), URL: https://linkinghub.elsevier.com/retrieve/pii/S0378381209002209.

[23] É.C. Lima, M.A. Adebayo, F.M. Machado, Kinetic and equilibrium models of adsorption, in: C.P. Bergmann, F.M. Machado (Eds.), Carbon Nanomaterials As Adsorbents for Environmental and Biological Applications, Springer International Publishing, Cham, 2015, pp. 33–69, http://dx.doi.org/10.1007/978-3-319-18875-1_3, URL: http://link.springer.com/10.1007/978-3-319-18875-1_3, Series Title, Carbon Nanostructures.

[24] M. Dubinin, V. Astakhov, Development of the concepts of volume filling of micropores in the adsorption of gases and vapors by microporous adsorbents, 1971, p. 5.

[25] W. Li, Z. Liu, S. Li, The optimal step locations for high-performance adsorption heat pumps under various working conditions, Therm. Sci. Eng. Prog. 25 (2021) 101033, http://dx.doi.org/10.1016/j.tsep.2021.101033, URL: https://linkinghub.elsevier.com/retrieve/pii/S2451904921001943.

[26] D.M. Ruthven, Principles of Adsorption and Adsorption Processes, Wiley, 1984.

[27] H.-J. Wang, A. Kleinhammes, T.P. McNicholas, J. Liu, Y. Wu, Water adsorption in nanoporous carbon characterized by in situ NMR: Measurements of pore size and pore size distribution, J. Phys. Chem. C 118 (16) (2014) 8474–8480, http://dx.doi.org/10.1021/jp501518f, URL: https://pubs.acs.org/doi/10.1021/jp501518f.

[28] J. Chun, S. Kang, N. Park, E.J. Park, X. Jin, K.-D. Kim, H.O. Seo, S.M. Lee, H.J. Kim, W.H. Kwon, Y.-K. Park, J.M. Kim, Y.D. Kim, S.U. Son, Metal–organic framework@microporous organic network: Hydrophobic adsorbents with a crystalline inner porosity, J. Am. Chem. Soc. 136 (19) (2014) 6786–6789, http://dx.doi.org/10.1021/ja500362w, URL: https://pubs.acs.org/doi/10.1021/ja500362w.

[29] K.C. Ng, M. Burhan, M.W. Shahzad, A.B. Ismail, A universal isotherm model to capture adsorption uptake and energy distribution of porous heterogeneous surface, Sci. Rep. 7 (1) (2017) 10634, http://dx.doi.org/10.1038/s41598-017-11156-6, URL: http://www.nature.com/articles/s41598-017-11156-6.

[30] O.J. Smith, A.W. Westerberg, The optimal design of pressure swing adsorption systems, Chem. Eng. Sci. 46 (12) (1991) 2967–2976, http://dx.doi.org/10.1016/0009-2509(91)85001-E, URL: https://linkinghub.elsevier.com/retrieve/pii/000925099185001E.

[31] L. Jiang, V.G. Fox, L.T. Biegler, Simulation and optimal design of multiple-bed pressure swing adsorption systems, AIChE J. 50 (11) (2004) 2904–2917, http://dx.doi.org/10.1002/aic.10223, URL: https://onlinelibrary.wiley.com/doi/10.1002/aic.10223.

[32] Q. Fu, H. Yan, Y. Shen, Y. Qin, D. Zhang, Y. Zhou, Optimal design and control of pressure swing adsorption process for N2/CH4 separation, J. Clean. Prod. 170 (2018) 704–714, http://dx.doi.org/10.1016/j.jclepro.2017.09.169, URL: https://linkinghub.elsevier.com/retrieve/pii/S0959652617321674.

[33] E. Sung, C.D. Han, H.-K. Rhee, Optimal design of multistage adsorption-bed systems, AIChE J. 25 (1) (1979) 87–100, http://dx.doi.org/10.1002/aic.690250110, URL: https://onlinelibrary.wiley.com/doi/10.1002/aic.690250110.

[34] F. Lanzerath, U. Bau, J. Seiler, A. Bardow, Optimal design of adsorption chillers based on a validated dynamic object-oriented model, Sci. Technol. Built Environ. 21 (3) (2015) 248–257, http://dx.doi.org/10.1080/10789669.2014.990337, URL: http://www.tandfonline.com/doi/full/10.1080/10789669.2014.990337.

[35] S. Galmarini, E. Piccoli, R. Civioc, S. Madry, V. Brancato, A. Frazzica, T. Nonnen, R. Herrmann, M. Koebel, Measuring Protocol for the Characterization of Adsorber Materials, Technical Report Hycool project D4.1, 2019, URL: https://hycool-project.eu/download/d4-1-measuring-protocol-for-the-characterization-of-adsorber-materials/.

[36] J.A. Nelder, R. Mead, A simplex method for function minimization, pp. 308–313, http://dx.doi.org/10.1093/comjnl/7.4.308, 7 (4), URL: http://comjnl.oxfordjournals.org/content/7/4/308.abstract.

[37] M. Rozwadowski, R. Wojsz, K.E. Wisniewski, J. Kornatowski, Description of adsorption equilibrium on type A zeolites with use of the Polanyi-Dubinin potential theory, Zeolites 9 (6) (1989) 503–508, http://dx.doi.org/10.1016/0144-2449(89)90045-6, URL: https://linkinghub.elsevier.com/retrieve/pii/0144244989900456.

[38] F. Stoeckli, Water adsorption in activated carbons of various degrees of oxidation described by the Dubinin equation, Carbon 40 (6) (2002) 969–971, http://dx.doi.org/10.1016/S0008-6223(02)00087-8.

[39] W. Wagner, A. Pruß, The IAPWS formulation 1995 for the thermodynamic properties of ordinary water substance for general and scientific use, 2002, pp. 387–535, http://dx.doi.org/10.1063/1.1461829, 31 (2) URL: http://aip.scitation.org/doi/10.1063/1.1461829.

[40] L.F. Velasco, R. Guillet-Nicolas, G. Dobos, M. Thommes, P. Lodewyckx, Towards a better understanding of water adsorption hysteresis in activated carbons by scanning isotherms, Carbon 96 (2016) 753–758, http://dx.doi.org/10.1016/j.carbon.2015.10.017, URL: https://linkinghub.elsevier.com/retrieve/pii/S0008622315303432.

[41] V.V. Kutarov, E. Robens, Y.I. Tarasevich, E.V. Aksenenko, Adsorption hysteresis at low relative pressures, Theor. Exp. Chem. 47 (3) (2011) 163–168, http://dx.doi.org/10.1007/s11237-011-9198-6, URL: http://link.springer.com/10.1007/s11237-011-9198-6.

[42] F. Pedregosa, G. Varoquaux, A. Gramfort, V. Michel, B. Thirion, O. Grisel, M. Blondel, P. Prettenhofer, R. Weiss, V. Dubourg, J. Vanderplas, A. Passos, D. Cournapeau, M. Brucher, M. Perrot, E. Duchesnay, Scikit-learn: Machine learning in Python, J. Mach. Learn. Res. 12 (2011) 2825–2830.

[43] C.S. Andreas Ruckstuhl, Robust fitting of nonlinear regression models, 2005.

[44] J. Ammann, B. Michel, P.W. Ruch, Characterization of transport limitations in SAPO-34 adsorbent coatings for adsorption heat pumps, Int. J. Heat Mass Transfer 129 (2019) 18–27, http://dx.doi.org/10.1016/j.ijheatmasstransfer.2018.09.053, URL: https://linkinghub.elsevier.com/retrieve/pii/S0017931018326310.

[45] Y.I. Aristov, I.S. Glaznev, I.S. Girnik, Optimization of adsorption dynamics in adsorptive chillers: Loose grains configuration, Energy 46 (1) (2012) 484–492, http://dx.doi.org/10.1016/j.energy.2012.08.001, URL: https://linkinghub.elsevier.com/retrieve/pii/S0360544212006135.

[46] U. Bau, P. Hoseinpoori, S. Graf, H. Schreiber, F. Lanzerath, C. Kirches, A. Bardow, Dynamic optimisation of adsorber-bed designs ensuring optimal control, Appl. Therm. Eng. 125 (2017) 1565–1576, http://dx.doi.org/10.1016/j.applthermaleng.2017.07.073, URL: http://www.sciencedirect.com/science/article/pii/S1359431117345349.

[47] S. Graf, F. Lanzerath, A. Sapienza, A. Frazzica, A. Freni, A. Bardow, Prediction of SCP and COP for adsorption heat pumps and chillers by combining the large-temperature-jump method and dynamic modeling, Appl. Therm. Eng. 98 (2016) 900–909, http://dx.doi.org/10.1016/j.applthermaleng.2015.12.002, URL: http://www.sciencedirect.com/science/article/pii/S1359431115013691.

[48] S. Samsatli, N.J. Samsatli, A general mixed integer linear programming model for the design and operation of integrated urban energy systems, 191, 2018, pp. 458–479, http://dx.doi.org/10.1016/j.jclepro.2018.04.198, URL: https://linkinghub.elsevier.com/retrieve/pii/S0959652618312344.

[49] H.G. Santos, T.A.M. Toffolo, Python - MIP, 2020, URL: https://pypi.org/project/mip/.

[50] A. Chakraborty, B.B. Saha, S. Koyama, K.C. Ng, K. Srinivasan, Adsorption thermodynamics of silica gel water systems, J. Chem. Eng. Data 54 (2) (2009) 448–452, http://dx.doi.org/10.1021/je800458k, URL: https://pubs.acs.org/doi/10.1021/je800458k.

[51] I. Jahan, M.A. Islam, M.L. Palash, K.A. Rocky, T.H. Rupam, B.B. Saha, Experimental study on the influence of metal doping on thermophysical properties of porous aluminum fumarate, Heat Transf. Eng. (2020) 1–10, http://dx.doi.org/10.1080/01457632.2020.1777005, URL: https://www.tandfonline.com/doi/full/10.1080/01457632.2020.1777005.

[52] B. Nienborg, S. Gschwander, G. Munz, D. Fröhlich, T. Helling, R. Horn, H. Weinläder, F. Klinker, P. Schossig, Life cycle assessment of thermal energy storage materials and components, Energy Procedia 155 (2018) 111–120, http://dx.doi.org/10.1016/j.egypro.2018.11.063, URL: https://linkinghub.elsevier.com/retrieve/pii/S1876610218310178.

[53] K. Uddin, Specific heat capacities of carbon-based adsorbents for adsorption heat pump application, Appl. Therm. Eng. (2018) 10.

[54] E. Toolbox, Water - Specific Heat (online), 2004, URL: https://www.engineeringtoolbox.com/specific-heat-capacity-water-d_660.html.

[55] S. Kayal, A. Chakraborty, H.W.B. Teo, Green synthesis and characterization of aluminium fumarate metal-organic framework for heat transformation applications, Mater. Lett. 221 (2018) 165–167, http://dx.doi.org/10.1016/j.matlet.2018.03.099, URL: https://linkinghub.elsevier.com/retrieve/pii/S0167577X18304634.

[56] L. Huber, P. Ruch, R. Hauert, G. Saucke, S.K. Matam, B. Michel, M.M. Koebel, Monolithic nitrogen-doped carbon as a water sorbent for high-performance adsorption cooling, RSC Adv. 6 (30) (2016) 25267–25278, http://dx.doi.org/10.1039/C6RA00548A, URL: http://xlink.rsc.org/?DOI=C6RA00548A.

[57] C. Schlüsener, M. Xhinovci, S.-J. Ernst, A. Schmitz, N. Tannert, C. Janiak, Solid-solution mixed-linker synthesis of isoreticular Al-based MOFs for an easy hydrophilicity tuning in water-sorption heat transformations, Chem. Mater. 31 (11) (2019) 4051–4062, http://dx.doi.org/10.1021/acs.chemmater.9b00617, URL: https://pubs.acs.org/doi/10.1021/acs.chemmater.9b00617.

[58] E. Piccoli, Water isotherms of adsorbent materials evaluated in the hycool project, Zenodo, 2022. http://dx.doi.org/10.5281/ZENODO.7093134. URL: https://zenodo.org/record/7093134.

[59] G. Restuccia, A. Freni, S. Vasta, Y. Aristov, Selective water sorbent for solid sorption chiller: Experimental results and modelling, Int. J. Refrig. 27 (3) (2004) 284–293, http://dx.doi.org/10.1016/j.ijrefrig.2003.09.003, URL: http://linkinghub.elsevier.com/retrieve/pii/S014070070300135X.

[60] S. AL-Hasni, R. Grant, G. Santori, The cost of manufacturing adsorption chillers, in: Heat Powered Cycles 2021, Bilbao, ES, 2022, pp. 138–148.